Indian Journal of Pure & Applied Physics
Vol. 63, November 2025, pp. 1003-1013
DOI: 10.56042/ijpap.v63i11.21715

Effects of Major Geomagnetic Storms on Total Electron Content near the Equatorial Ionization Anomaly (EIA) and Low Latitude Regions

Vishakha[a], Vishal Chauhan[a*] & Rakesh Singh[b]

[a]Department of Physics, Graphic Era Hill University, Dehradun 248 002, India

[b]Department of Petroleum Engineering, Graphic Era (Deemed to be University), Dehradun 248 002, India

Received:18th July 2025; accepted:6th October 2025

In this paper, we investigated the fluctuations in Total Electron Content (TEC) during major geomagnetic storms from 2012 to 2021, using the data from six IGS stations: GUAM, GUUG, IISC, DARW, KAT1, and ALIC. We studied the effect of six major geomagnetic storms on TEC, which occurred on 8 September 2017, 17 March 2015, 15 July2012, 8 May 2016, 7 October 2015, and 20 December 2015. These events showed substantial variations in TEC, with noticeable increases from 2.4% to 346%. We also used the global aTEC maps to demonstrate the spatial diversity of TEC enhancements. The analysis indicated that the most significant TEC variations occurred in equatorial and low-latitude regions.The stations located near the equator region responded earlier to the geomagnetic storms of 17 March 2015, 20 December 2015, 8 May 2016. Further, the ionospheric effects are found to be subsequently shifting toward low-latitude stations due to the equatorial electrodynamics and prompt penetration electric fields (PPEF). However,during the geomagnetic storm of15 July 2012 the low latitude stations responded earlierthan equatorial stations. The findings emphasize the crucial role of geomagnetic activity in driving changes in the ionosphere, which in turn affects global TEC levels.

Keywords:TEC, EIA, Geomagnetic storm, Ionosphere, EEJ

1 Introduction

Geomagnetic storms are the major disruption of the earth's magnetic field. It happens when the atmospheres of the Sun and the Earth perfectly inter change energy. The frequency of magnetic storms fluctuates with the sunspot cycle. Geomagnetic storm occurs more often during solar maximum with majority by coronal mass ejections (CMEs). These storms are caused by a variety of solar wind that produces dramatic changes in current plasma and field in earth's magnetosphere[1-4]. Large geomagnetic storms can be harmful to ground and space-based installations. Major geomagnetic disturbances can have disruptive effects like losing satellite signals, breaking down communication networks, and disruptive electric power grids in addition to creating stunning auroral displays in the northern and southern hemispheres[5-7]. The use of Global Positioning System (GPS) for monitoring the ionosphere has become prevalent on a regional and worldwide basis. GPS is a very useful instrument for investigating ionospheric structures because of its ongoing operations and global network of receivers. This technique is particularly crucial during the times of geomagnetic disturbances, when the dynamics and energy dissipation processes within the magnetosphere, thermosphere, and ionosphere system become extremely complex. One of the primary parameters derived from GPS data is the total electron content (TEC), which measures the number of electrons between a GPS satellite and a receiver. TEC is an essential metric in evaluating ionospheric variability and is instrumental in recognizing and predicting space weather impacts.

This significance is particularly apparent in the equatorial and low-latitude regions, in which ionospheric processes are dynamic and complex. Processes like the equatorials spread-F (ESF), equatorial electrojet (EEJ), and equatorial ionization anomaly (EIA) are some key characteristics in these areas. Due to these distinctive and generally unpredictable properties, ionospheric studies groups have turned these areas into a primary area of focus to develop a better understanding of ionospheric processes and to enhance predictive models through TEC data. The densely populated equatorial ionosphere is identified by the EIA & enhanced ionization approximately ±15 ° of the magnetic

*Corresponding author: E-mail: vishalchauhan@gehu.ac.in

equator[8,9]. Strong anomalies that greatly affect GPS performance are common in this area. The formation of the EIA, EEJ, and ionospheric abnormalities are all greatly influenced by the equatorial electric field, which is a major factor driving the electrodynamics of the equatorial ionosphere[10]. The formation of irregularities is enabled by the increased electric field, which redistributes ionization in the area of the EIA crests and raises the F-layer to higher altitudes where recombination is less common[11]. Trivedi et al. (2011) examined the variations in TECduring geomagnetic storms with Dst< -50 nT (reaching -300 nT) from 2005 to 2007 using GPS satellite data in Bhopal, India (23.16 ° N, 77.36° E). According to the study, vertical TEC (VTEC) experienced a positive percent deviation during the storm's main phase. This was caused by the prompts penetration electric fields (PPEF)) due to under and over-shielding. PPEFs are electric fields that change the distribution of ionospheric plasma during geomagnetic storms by moving rapidly from the magnetosphere into the ionosphere. VTEC showed both positive and negative variances throughout the recovery period[12]. Oikonomou *et al*. (2022) used data from ten European locations to examine the negative ionospheric responses during two storms on 8 September 2017. Due to several mechanisms, the study identified unique characteristics for every storm. They observed that the electron density decrement was linked to themidlatitude Ionospheric Trough (MIT) displacement, with regional variations between northern and southern Europe[13]. Lissa *et al*. (2022) studied the effects of magnetic storms occurred on 20 January, 6 March, and 13 October, 2016. They observed the Symmetric-Horizontal index (SYM H) values dropped with lowest of -95 nT and -114 nT. Their study found that storm-induced electric field changes and an increased O/N2 ratio in the thermosphere contribute to the positive storm effect. This effect was observed during the recovery phases of the storms on 6 March and 13 October. A significant positive storm effect was noted after the 13 October storm, produced by Co-rotating Interaction Regions (CIR) disturbances.CIR are solar wind structures that is formed by fast solar wind overtaking slower wind and causing the geomagnetic disturbances[14]. Tariq *et al*. (2022) investigated the GNSS-derived TEC during two strong magnetic storms in May and September 2017 and found a longitudinal dependence of ionospheric responses. During the main phase, on 28 May they observed TEC enhancement caused bythe southward direction turning of the Interplanetary Magnetic Field (IMF) and eastward direction of PPEF. On 29 May, at the time of the recovery, the ionospheric variations were triggered by later southward IMF-Bz turning in the Asian regions, with negative ionospheric storm responses observed on 30 May. On 8 September 2017, they recorded, the TECvalues increaseduring the period of main phase of the storms[15]. Jenam *et al*., (2021) studied the ionospheric TEC responses to the September 2017 geomagnetic storm and December 2019 annular solar eclipse. They observed the TEC variation over the regions of Sri Lankan, equatorial and low latitude regions. When a significant magnetic storm accompanied with a solar flare occurred in September 2017, they observed a positive ionospheric storm effect. A change of 11 TECU was observed by them during the main phase of the storm. During the recovery phase, the disturbance dynamic electric field comes after the PPEF[16].

To investigate the ionosphere's response to magnetic storms, we selected six cases of geomagnetic storms ($\sum K_p \geq 45$) which occurred on 8 September 2017 ($\sum K_p = 49$), 17 March 2015 ($\sum K_p = 48$), 15 July 2012 ($\sum K_p = 47$), 8 May 2016 ($\sum K_p = 46$), 7 October 2015 ($\sum K_p = 45$), and 20 December 2015 ($\sum K_p = 45$). The further sections cover the specifics of TEC and geomagnetic parameter changes during these storms time.

2 Method

In this study we used the GPS data from six International GNSS service (IGS) stations, ALIC (Australia), KAT1 (Australia), DARW (Australia), IISC (India), GUUG (Mangilao USA), and GUAM (Guam). Their locations and coordinates are given in Table 1. The locations of the stations on the world map are shown in Fig 1.

These stations are selected on the basis oftheir geographical location and availability of continuous data of GPS TEC from the IGS database. The GPS data from the IGS stations are processed to get TEC values, indicative of ionospheric disturbances. It can be expressed as the total number of electrons along a radio wave's path or the line integral of electrons density Ne (l) along a ray path.The TEC is measured in TECU andone TECU is equal to 10^{16} electrons per meter^2. TEC can be estimated more precisely with a dual frequency GPS receiver, which operates at frequencies of 1227.60 MHz and 1575.42 MHz. The TEC is calculated by using the formula

Table 1 — Details of stations and their Geographical location

S.No	Station code	Country	Geographic Latitude	Geographic Longitude
1.	GUAM	Guam	13.589	144.868
2.	GUUG	Mangilao, USA	13.433	144.803
3.	IISC	India	13.021	77.570
4.	DARW	Australia	-12.844	131.133
5.	KAT1	Australia	-14.376	132.153
6.	ALIC	Australia	-23.670	133.886

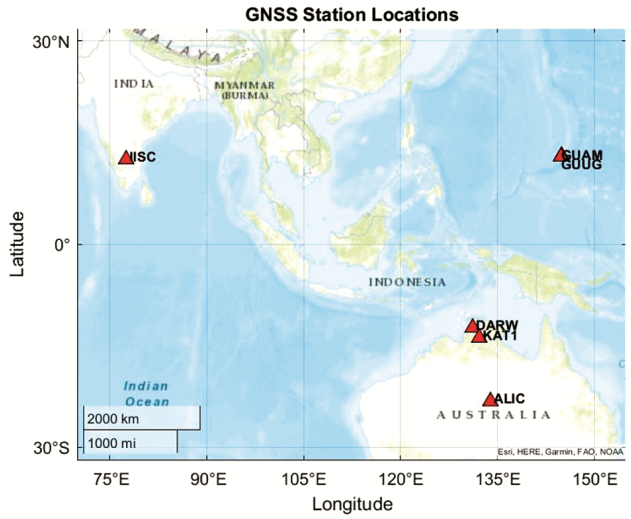

Fig. 1 — Geographic locations of six IGS station i.e, ALIC, KAT1, DARW, IISC, GUUG, and GUAM

$$TEC = \frac{1}{40.33}\left(\frac{f_1^2 f_2^2}{f_1^2 - f_2^2}\right)(P2 - P1) \quad \ldots (1)$$

Marković (2014) and Stankov *et al.* (2001) gives the details of calculation and explanation of TEC[17,18]. The Vertical TEC has been derived from the GPS observation in RINEX format. To obtain VTEC, we used the software developed by GopiSeemala.

To investigate the magnetic storm effect on GPS derivedionospheric TEC, we considered six significant geomagnetic storm events ($\sum K_p \geq 45$) which occurred on 8 September 2017 ($\sum K_p = 49$), 17 March 2015 ($\sum K_p = 48$), 15 July 2012 ($\sum K_p = 47$), 8 May 2016 ($\sum K_p = 46$), 7 October 2015 ($\sum K_p = 45$), and 20 December 2015 ($\sum K_p = 45$). The global response of geomagnetic storms is observed from the geomagnetic indices, including Kp index and Dst index. The Kp index provides the strength of the disruption in the Earth's magnetic field's horizontal component every three hours. It is measuring geomagnetic activity in the sub-auroral regions. It's values varies from 0 to 9, with a number greater than 4 indicating the occurrence of a geomagnetic storm[19]. The Dst index is a measure of the strength of the ring current around the Earth, expressed in nanotesla (nT)[20]. The westward drift of the proton determines the direction of the ring current. Dst values arer ecorded hourly. This measure is used to identify a geomagnetic storm's initial, main, and recovery phases. A quick rise in Dst indicates the storm's first phase, also known as its sudden onset. This is followed by a sharp decline during the main phase and a slow rise towards the undisturbed condition during the recovery phase. A geomagnetic storm is considered to occur when Dst ≤ –50 nT, while intense or severe storms are typically defined by Dst ≤ –100 nT.The Kp and Dst data are taken from World Data Centre (WDC) for Geomagnetism, KYOTO Japan.

We also used GNSS-derived global TEC (gTEC) maps to observe spatial TEC fluctuations, with a focus on the equatorial area. There are four different types of 2-D maps namely, absolute TEC (aTEC) maps, ratio of TEC difference (rTEC) maps, detrended TEC(dTEC maps) and rate of TEC index (ROTI) maps that have been created using geographic coordinates with 10-minute time intervals using RINEX files. In this paper, we used aTEC maps to observe the global response of TEC related to different geomagnetic storms.

3 Results and Discussion

As described in Section 2, in this part, we concentrate on the analysis of geomagnetic storm events based on VTEC observations at six locations. For the analysis, we considered particular storm events to study their influence on the behavior of the ionosphere. A detailed analysis of each storm event has been made to comprehend the ionospheric response at various phases of the storm. We also discussed the global variation in TEC through global maps of TEC to understand the spatial coverage of ionospheric perturbations. The results of each event are described separately in the subsequent subsections.

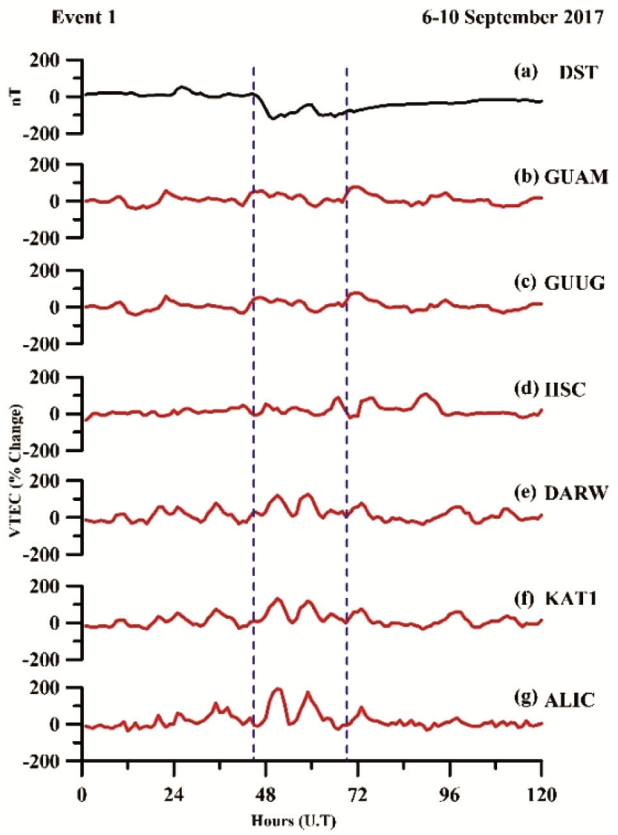

Fig. 2 — Variation of Dst index and maximum percentage inVTEC at stations ALIC, KAT1, DARW, IISC, GUUG, and GUAM during 6–10 September 2017, dashed line (event-day VTEC)

3.1 The storm of 8 September 2017

The variations of VTEC during the September 2017 geomagnetic storm are investigated utilizing observations from six ground-based GPS stations. For illustration, Fig. 2 shows the Dst index (a) and the percentage change variations of VTEC (b-g) at six stations, ALIC, KAT1, DARW, IISC, GUUG, and GUAM respectively for 6–10 September 2017.

For this analysis, we used hourly VTEC data to capture short-time variations as well as to better define the ionospheric response.The observations of five days percentage change variation in VTEC revealed distinct patterns of fluctuation over the stations. It can be seen from Fig. 2 (a), the values of Dst indices started fluctuating mildly around a stable range indicating calm magnetic conditions. However, during the event period of 8 September, the Dst values exhibits a major drop reaching a minimum approximately -122 nT at 0200 hours (h) Universal Time (UT), signifying a geomagnetic storm. This sharp decline reflects heightened geomagnetic disturbance, likely triggered by a solar storm or a

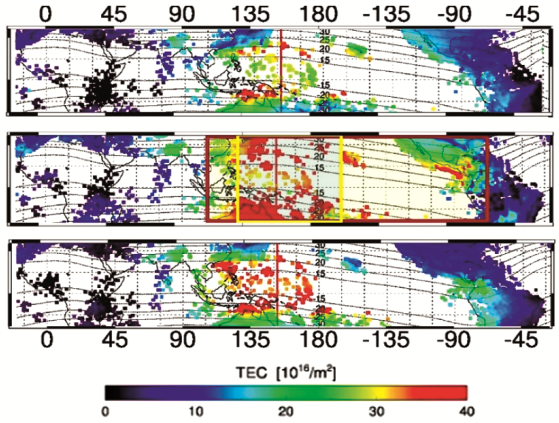

Fig. 3 — The aTEC maps corresponding to the geomagnetic storm of 8 September, 2017 from 7-9 September 2017 at 0150 h UTC. The yellow and red rectangles are highlighting the anomalous aTEC values

similar space weather phenomenon. Following the event, the Dst index gradually returns to its baseline values, indicating the geomagnetic field's stabilization and recovery. The ionospheric response, which measured in percentage change in VTEC over five days, also noted. The initial phase of the storm was started on 7 September 2017. During main phase on 8 September marked by vertical blue coloured dashedline the storm peak noted at around 0300 UT at station ALIC, KAT1 and DARW with maximum percentage change of 176 %, 117.6 % and 109.6 % respectively. This early response indicates that the stations are near equator, and low-latitude ionosphere and the geomagnetic disturbance in these areas are quickly coupling. Additionally, the disturbances at IISC, GUUG, and GUAM, occurring comparatively later, areshowing VTEC changesof 68 %, 73 %, and 71.6 %, respectively. The delayed response of magnetic storms at these locations may be due to the spatial variations in ionospheric dynamics, such as the impact of storm-time electric fields, thermospheric winds, and travelling ionospheric disturbances (TIDs). To substantiate this localized observation, a global overview is givenby showing the global TEC maps of three successive days, i.e. 7 to 9 September at 0150 h UT. These maps, depicted in Fig. 3, concentrate on the equatorial and low-latitude zones in the -30 ° to 30 ° latitude range.

Two geographical regions are specified: a red rectangle between 105 ° to -75 ° longitude, exhibiting moderate enhancements of 20 to 40 TECU, and a yellow rectangle between 120 ° to 180 ° longitude, where larger enhancements are noted with the value

peaking at 40 TECU. These enhancements reflect greater intensification of the ionospheric disturbance caused by the geomagnetic storm. Differences among these regions reflect the varied intensities of interaction between the storm and Earth's magnetic field, resulting in greater disturbances in the yellow-colored region. Thecolor scale in the maps ranges between darker blue (smaller TEC value) and bright red (higher TEC values), pictorially representing the spatial distribution of the ionospheric response during the storm event.

3.2 Event 2: The storm of 17 March 2015

The second geomagnetic storm of 17 March 2015, is also known as St. Patrick's Day Storm. The main cause of this storm was CME linked to a C9-class solar flare that erupted from active region AR2297 on 15 March, 2015. The fact that this CME was Earth-directed and showed up in coronagraph images as a complete halo indicates it was strongly launched in the direction of Earth. Early on March 17, 2015, the CME entered Earth's magnetosphere after spending around two days in interplanetary space. To study and analyse the storm progression and ionosphere response at different regions, we plotted the Dst and VTEC percentage change during the period 15 to 19 March, 2015 as shown in Fig. 4.

It can be seen from top panel of Figure, the Dst index starting at around 1nT indicating quiet geomagnetic conditions initially. During the event time of 17 March, a significant change in Dst was observed. The Dst index going decreases from 0800 – 2400h UT. At 0800 UTC its values dropped -18 nT and at 2300h UT the value was -234 nT. This substantial drop in Dst index signifies a strong magnetic storm. In the recovery phase the Dst index exhibits a minor drop reached approximately -70 nT. The geomagnetic storm onset time is around 04:45 UTC on 17 March 2015 distinguished by sudden direct impact of the CME on Earth's magnetosphere. The storm gradually increased during the day to maximum at about 23:00 UTC when the Dstindex dropped to its lowest value (−234 nT). Ionospheric responses corresponding to those above are evident in the VTEC data recorded at the different GNSS stations. One of the stations showed maximum percentage change in VTEC of approximately 115 % indicating a significant positive storm effect during the main phase of the event. This enhancement of electron content is associated with the penetration of storm-time electric fields and the disturbed state of thermospheric dynamics. During the backside of the storm, the recovery phase

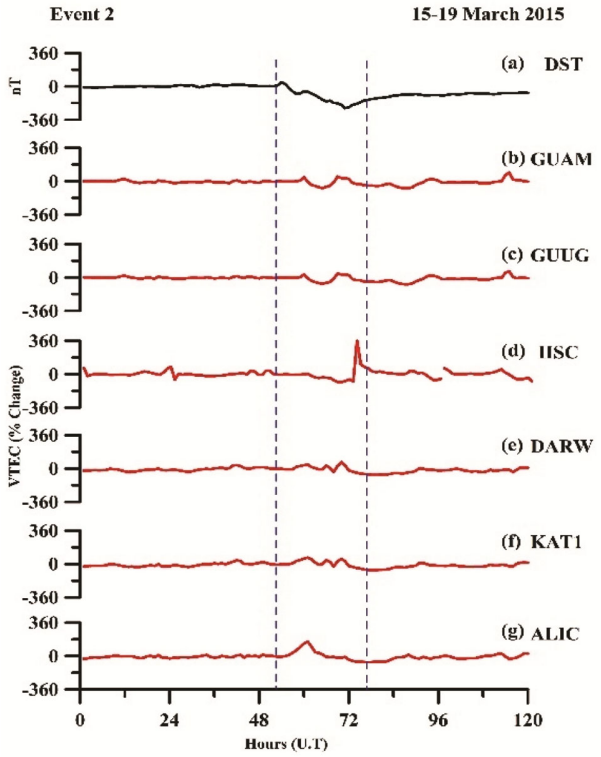

Fig. 4 — Variation of Dst index and maximum percentage inVTEC at stations ALIC, KAT1, DARW, IISC, GUUG, and GUAM during 15-19 March 2015, dashed line (event-day VTEC)

started, with the geomagnetic condition returning back to normal gradually. This recovery continued through into 19 March 2015, where the Dst index and VTEC values started to head back to quiet time levels. These observations, altogether, show the close coupling between geomagnetic perturbations and ionospheric variability around the 17 March 2015 storm. The $\sum K_p$ indices also observed over a five days period from 15-19 March were 14, 19, 48, 39 and 30 respectively. The $\sum K_p$ index reached 48 on 17 March, the highest value compared to all prior days, indicating strong magnetic disruptions. This high $\sum K_p$ index, which reflects disruptions in the Earth's magnetic field, which is a sign of significant geomagnetic activity. These elevated values are usually associated with geomagnetic storms, which can affect satellite operations and communication systems in several ways. The ionospheric response seen in Fig. 5, which shows global TEC changes during the storm, enhances this significant geomagnetic activity.

The peak occurrence on 17 March, the regions of maximum impact by the storm, between -30 ° and 15 ° latitude and -75 ° and -45 ° longitude, are identified by yellow rectangles, where the TEC

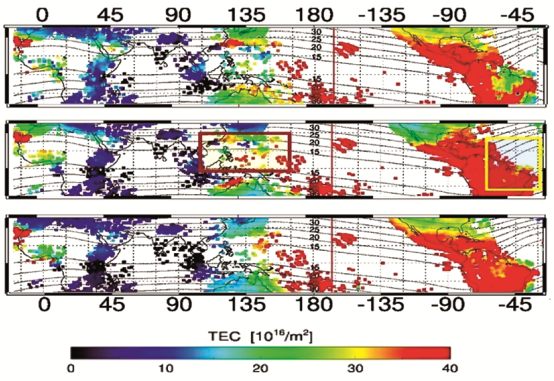

Fig. 5 — The aTEC maps corresponding to the geomagnetic storm of 17 March 2015 from 16-18 March 2015 at 2300 h UTC

readings significantly increased to as high as 40 TECU. Conversely, the regions colored in red rectangles from -25 ° to 15 ° latitude and 105° to 165° longitude recorded TEC variations between 30 to 40 TECU, in comparison to the other days.

3.3 The storm of 15 July 2012

On 12 July, 2012 a strong X1.4 class solar flare erupted from the active region 1520 of the Sun's surface. This flare was followed by a rapid halo coronal mass ejection (CME) observed first in LASCO C2 coronagraph at 16:48:05 UT. The plane-of-sky velocity of the CME was about 885 km/s with peak velocities of 1415 km/s. The event was linked to a complex magnetic structure referred to as a double-decker magnetic flux rope which was formed by shearing and converging motions at the magnetic foot points of the active region. Such an arrangement was part of the reason that the CME was intense and geoeffective[21]. On 15 July, 2012, the CME reached on Earth, causing a G3-class geomagnetic storm, according to NOAA.To analyze the ionospheric response to the geomagnetic storm of 15 July 2012, the Dst index and VTEC variations are examined over a five-day period from 13 to 17 July 2012, as shown in Fig. 6.

As seen from the top panel, the Dst values shows the variations throughout the period of 120 hours. The Dst index shows stable geomagnetic conditions at first since it is largely stable and stays close to a neutral value. After the 0400h UT the Dst values starts to decreases indicating the beginning of geomagnetic storm activity.The Dst index experiences a large decrease at the 1800-2000 h UT, with a minimum value of about -139 nT. This indicates the end of a period of severe geomagnetic disruption and the

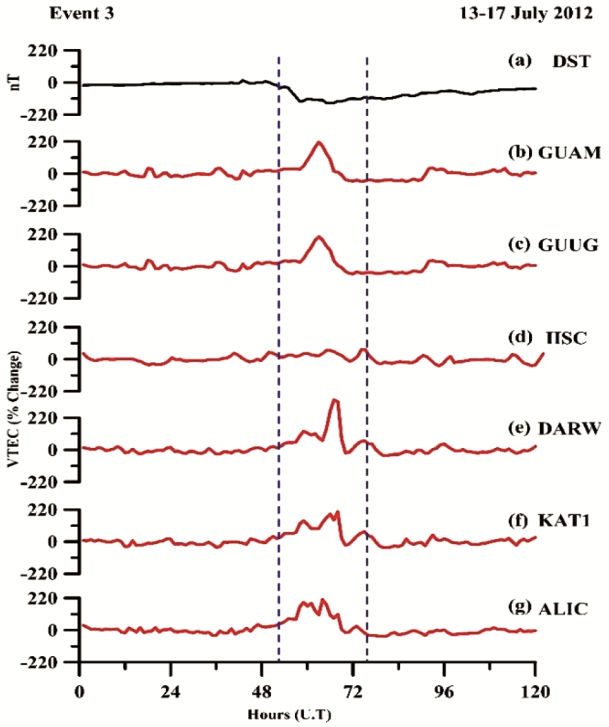

Fig. 6 — Variation of Dst index and maximum percentage inVTEC at stations ALIC, KAT1, DARW, IISC, GUUG, and GUAM during 13-17 July 2012, dashed line (event-day VTEC)

peak of the geomagnetic storm. The geomagnetic disturbances continue on next day during 0100-1100 h UT, but after that, the Dst values progressively return to normal, signifying the stabilization and recovery of the Earth's magnetic field. The$\sum K_p$values from 13 to 17 July are 3, 19, 47, 36 and 23. The $\sum K_p$ index reached 47 on 15 July, that indicating strong magnetic disruptions.On the same day, large VTEC enhancements aredetected at all six stations. The maximum percentage of VTEC at stations that are near the equator shows more TEC enhancements, then it shifts to upper latitude side stations. The maximum percentage changes observed were 203 %, 197 %, 346 %, 64.2 %, 204 % and 191 % respectively. More insight in the global effects of the storm is given by the a TEC maps in Fig. 7, which present the spatial distribution of TEC over three days between 14 and 16 July 2012.

These global maps taken at 1700 h UT show large variations in TEC, particularly in regions between -30 ° to 30 ° latitude and 45 ° to 180 ° longitude, as indicated by red rectangles. Within the red rectangle between longitude 120 ° and 165 ° and latitude -30 ° and 15 °, enhancements of 20 to 25 TECU occurred. Within a further region between longitude -120° to -

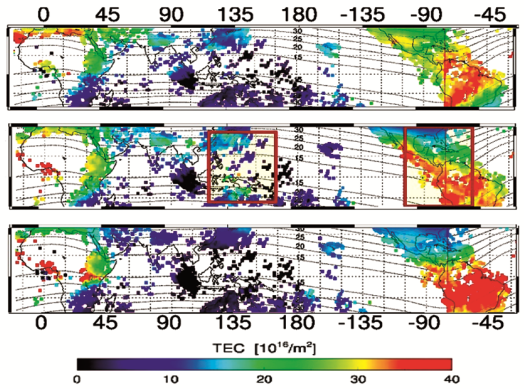

Fig 7 — The aTEC maps corresponding to the geomagnetic storm of 15 July 2012 from 14-16 July 2012 at 1700 h UTC

75° and latitude -25° to 30° latitude, the TEC was even larger, between 35 and 40 TECU.

3.4 The storm of 08 May 2016

The geomagnetic storm on 08 May was observed beginning at 0259 h UT due to an enhanced solar wind environment. A CME was triggered and reached on earth on 8 May. To analyse the ionospheric variation, we plotted the Dst and VTEC percentage change in Fig. 8. This figure shows the variation of Dst and VTEC during 06 -10 May 2016 at station GUAM, GUUG, IISC, DARW, KAT1 and ALIC.

As seen from top panel the Dst indices baselines reading show consistent quiet geomagnetic conditions during the starting days but on 8 May the DST values, show a significant decline during 0800-0900 h UT, with a minimum of -95nT indicating the presence of a geomagnetic storm. On 9 May the geomagnetic field is little stabilising and recovering on 10 May, as the DST index progressively returns to its baseline values. The corresponding $\sum K_p$ values from 6-10 Maywere 22, 16, 46, 31 and 22. $\sum K_p$ values were maximum on 8 May that indicate the geomagnetic disturbances. It is observed that, during the main phase of the storm (0800-0900 UTC) the station ALIC, KAT, DARW responding disturbances immediately after the onset time (5:59 UTC). The maximum percentage changes observed 150 %, 160 %, 128 % and the station IISC, GUUG, GUAM shows disturbances during the main phase with 137 %, 27.5 % and 34.6 % respectively. This study shows the ionosphere responds to a geomagnetic storm both temporally and spatially. It is clearly observed that the station at southern region (ALIC, KAT, DARW) shows early disturbances and followed by notable increases at northern equatorial and

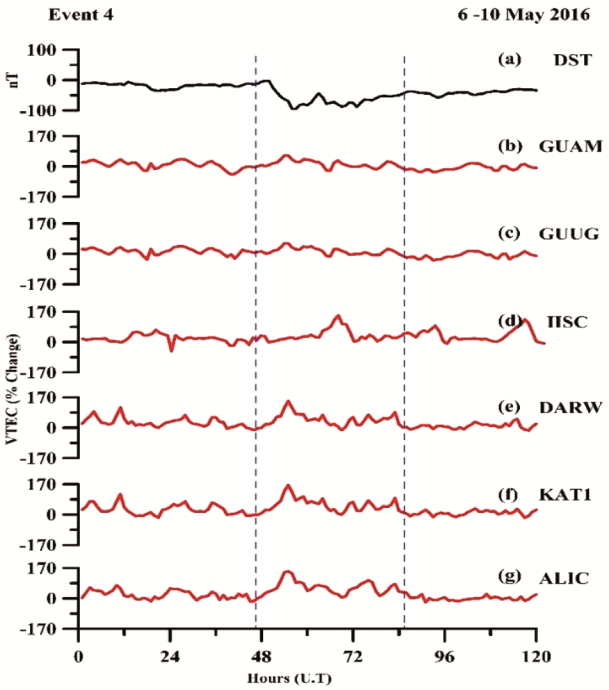

Fig 8 — Variation of Dst index and maximum percentage inVTEC at stations ALIC, KAT1, DARW, IISC, GUUG, and GUAM during 6-10 May 2016, dashed line (event-day VTEC)

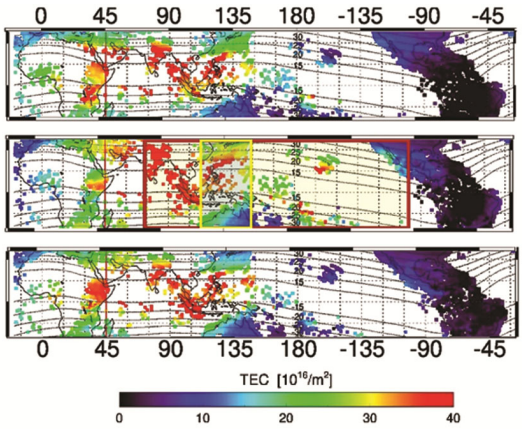

Fig 9 — The aTEC maps corresponding to the geomagnetic storm of 8 May 2016 from 7-9 May at 0900 h UTC

mid-latitude stations.These results further confirm the widespread ionospheric impact of the geomagnetic storm across different latitudinal regions.

These results are consistent with the global aTEC variations depicted in the map in Fig. 9, which depicts 7–9 May 0900 h UT data.

On 8 May, the map records evident enhancements in TEC in two regions defined by red and yellow rectangles. The red rectangle between latitudes -30 ° to 30 ° and 75 ° to -105 ° longitude records enhancements in 20 to 40 TECU, whereas in the

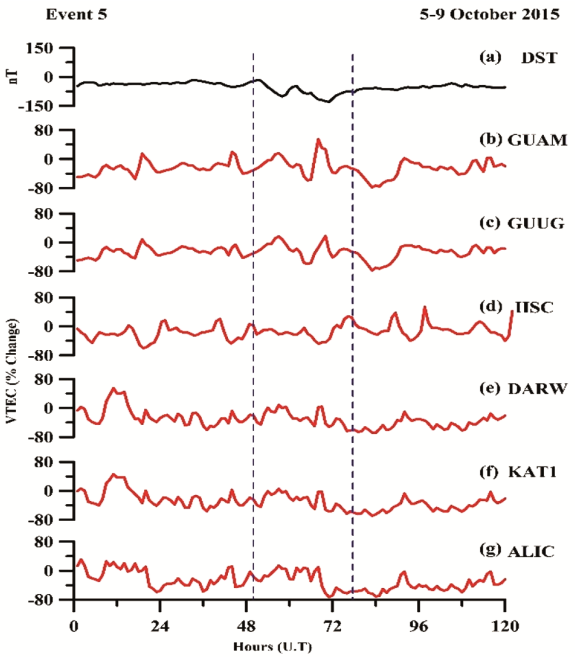

Fig 10 — Variation of Dst index and maximum percentage inVTEC at stations ALIC, KAT1, DARW, IISC, GUUG, and GUAM during 5-9 October 2015, dashed line (event-day VTEC)

yellow-marked sector between -30° to 30° latitudes and 105° to 150° longitude, slightly elevated TECs of 30 to 40 TECU are observed.

3.5 The storm of 07 October 2015

A CME is the main cause of the magnetic storms that occurred on 7 October, 2015, involved the expulsion of magnetic field and plasma from the Sun's corona. The Earth's magnetosphere affected by these ejections after they arrive, causing geomagnetic storms. For this study, Dst and VTEC data are analyzed for five days, from 5 to 9 October, 2015 at six stations: GUAM, GUUG, IISC, DARW, KAT1, and ALIC in Fig. 10. As shown in the top panel of the figure, Dst values are stable on 5 and 6 October, indicating quiet conditions. On 7 October, the Dst index dropped sharply, reaching -101 nT at 1000 h UT and -130 nT by 2300 h UT, marking the peak of the geomagnetic storm. On 8 and 9 October, Dst values started to return to normal, showing the recovery phase. The $\sum K_p$ values during this period were 24, 25, 45, 39, and 31, with the highest value (45) on 7 October, confirming strong geomagnetic activity.The storm began at 6:00 UTC, and the steep decline in the Dst index around 2300 UTC marked the maximum geomagnetic disturbance.

Significant variations are seen at all six IGS stations. The highest percentage change in VTEC is

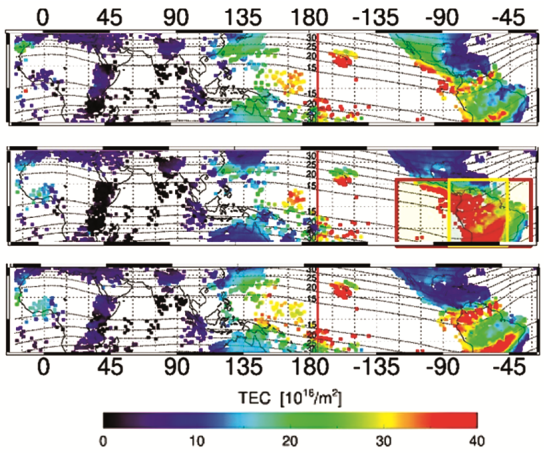

Fig 11 — The aTEC maps corresponding to the geomagnetic storm of 7 October 2015 from 6-8 October at 2340 h UTC

49.1%. The recovery phase continued until 8 October, when the geomagnetic conditions calmed down and the VTEC fluctuation started to stabilise.

The station in southern region responds ionospheric disturbances first that indicate the early penetration of geomagnetic field disturbances. The difference in time and space may be due to disturbance dynamo effects and prompt penetration electric fields (PPEFs), which have varying effects on ionospheric plasma at different latitudes. The disturbance's abrupt equatorward shift indicates a link between low-latitude ionospheric dynamics and high-latitude magnetospheric activities.These results are further supported by the global aTEC map shownin Fig. 11, which presents the variations of TEC over the three-days from 6–8 October at 2340 h UT.

The marked increases of the TEC are prominent in two specific regions indicated by red and yellow rectangles. The red-colored box, stretching across latitudes -30° to 15° and longitudes -120° to -30°, indicates increases in the range of 20–40 TECU. On the other hand, the yellow-marked box between latitudes -30° to -15° and -90° to -45° shows slightly greater increases in the range of 35–40 TECU.

3.6 The storm of 20 December 2015

On 20 and 21 December, 2015, two CMEs entered the earth's magnetosphere and created a powerful geomagnetic storm that NOAA rated as a G3 storm. For this study the data of Dst and VTEC areanalyzed from 18 to 22 December choosing the stations GUAM, GUUG, IISC, DARW, KAT1 and ALIC. The results are presented in Fig. 12.

The uppermost panel of the plot indicates the Dst index starting to fall by 1000 h UT on 20 December and reaching a minimum value of -166 nT by 2300 h UT, signifying the principal stage of the geomagnetic storm. On 21 December, Dst was low, indicating the persistent effects of the storm, and a gradual recovery was noticed starting on 22 December. The corresponding $\sum K_p$ index from 18–22 December were 9, 15, 45, 31, and 20, the largest value occurring on 20 December, affirming extensive geomagnetic disturbances on that day. The maximum percentage changes during the geomagnetic storms are given in Table 2.

These unusually high rises signify robust ionospheric responses in various latitudinal regions. Fig. 13 is showing the global distribution of aTEC for 19–21 December at 2300 h UT which emphasizes the response of the ionosphere during the geomagnetic disturbance.

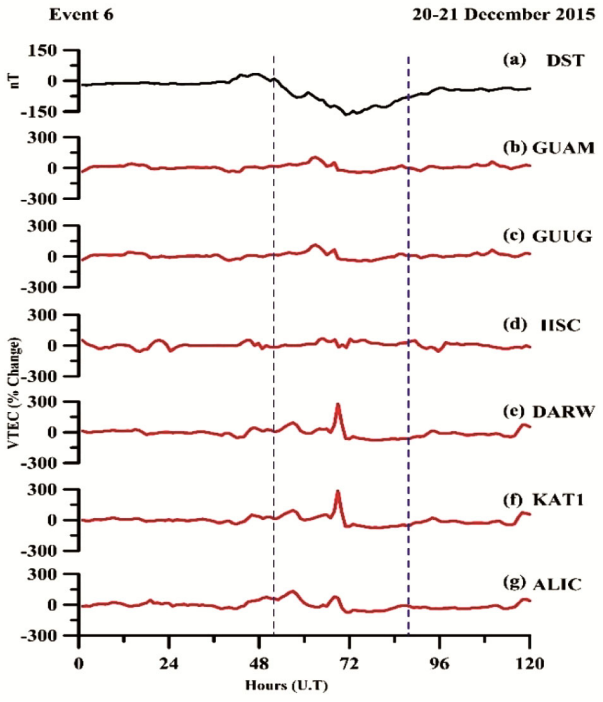

Fig 12 — Variation of Dst index and maximum percentage inVTEC at stations ALIC, KAT1, DARW, IISC, GUUG, and GUAM during 18-22 December 2015, dashed line (event-day VTEC)

On 20 December, red and yellow-colored regions depict the strong enhancements in the TEC. The red box, covering latitudes -30° to 30° and longitudes -120° to -30°, indicates increases in the TEC of up to 30 TECU. On the contrary, the yellow box, covering latitudes -30° to 15° and -90° to -60° longitudes, depicts even greater enhancements of 40 TECU. These high levels of the TEC suggest increased ionization and electron density due to the effects of geomagnetic disturbances. Compared to the neighbouring days 19 and 21 December the enhancements are clearly more pronounced.

We analysed the six major geomagnetic storms cases and observed that the events 1,3 and 4 (8 September 2017, 15 July 2012, and 8 May 2016 respectively) showed similar and positive ionospheric response.The VTEC enhancements alsoobserved at low latitude and equatorial regions.The enhancements are mainly due to PPEFs, which strengthened the EIA by intensifying upward plasma drift through E × B processes. Further more, during these periods, the EEJ was strengthened, which contributed to further uplift and redistribute ionospheric plasma.These findings are in agreement with prior studies. For example, Paul *et al*. (2020) investigated the effects of the 20 December 2015, geomagnetic storm on the TEC response over mid- and low-latitude stations. During

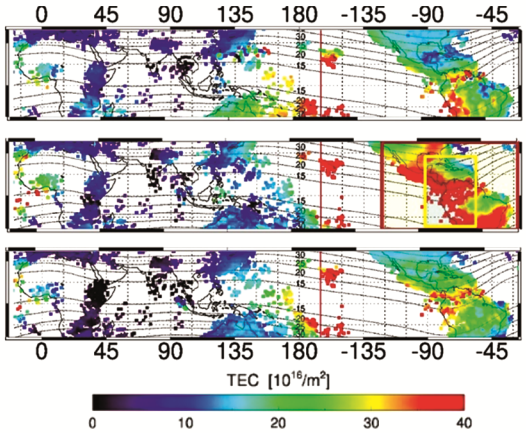

Fig 13 — The aTEC maps corresponding to the geomagnetic storm of 20 December 2015 from 19-21 December at 2300 h UTC

Table — 2 Maximum Percentage change during event time for all stations

Events	GUAM%	GUUG%	IISC%	DARW%	KAT1%	ALIC%
08 Sep 2017	71.6	73	68	109 - 6	117.6	176
17 Mar 2015	55.3	58.6	36.4	49.6	64	115
15July 2012	191	204	64.2	346	197	203
08 May 2016	34.6	27.5	137	128	160	150
07 Oct 2015	49.1	12.9	23.3	2.8	2.4	9.8
20 Dec 2015	107.4	109.8	57	241	268	96

the storm's main phase, they found a significant TEC variation at low and mid-latitudes caused by the PPEF[22]. Sharma *et al*. (2011) noted that during the magnetic storm on 24 August, 2005, at Bengaluru, the anomalous plasma fountain originating from the first PPEF and this electric field caused the Enhancement of TEC to increase by this factor[23]. Galav *et al*. (2012) studied a magnetic storm that was happened on 30 May 2005 and at station Bengaluru they observed that the TEC values increased 60 percent[24]. Lissa *et al*. (2020) investigated the ionosphere's responses at the low and equatorial regions of the severe magnetic storm on 26 August, 2018, using GPS stations. Along with the significantly increased ratio of thermosphere neutral composition, they also noted that the effect of storm is positive throughout the recovery and main phase, which was ascribed to the eastward PPEF. Geomagnetic storm on 15 July 2012 results shows someother factorsare contributed including thermosphericheating and solar illumination[25].

The event 2 (17 March 2015), however, shows a similar pattern, with PPEF effects occurring but not consistently across all stations,while, Event 6 (20 December 2015) had variability in addition to regional enhancement, as Mansilla *et al*. (2020) results supports our results. They studied the foF2 and hmF2 of the F2 layers at equatorial and low-latitude stations in the South American region during the geomagnetic storm occurring from 19–22 December 2015. They observed a reduction in foF2 initially at equatorial and low latitudes, particularly over the northern crest of the EIA, while the southern crest was minimally affected. This initial decrement during the storm is to be caused by the westward electric field penetration. Elevated upward vertical drift at equatorial latitudes may intensify the fountain effect and cause the subsequent positive effects seen during the storm's main phase. Variations in the O/N2 ratio most certainly played a role in both the positive and negative impacts seen throughout the storm's recovery phase[26]. Amaechi *et al*. (2018) studied the effects of severe magnetic storms of 2015 on TEC over the regions of African, equatoriallow-latitude. The magnetic storm occurred in December 2015, they observed the impact of the electric field was insignificant during the storm December 2015. During the storm's recovery phase, these abnormalities were effectively suppressed by westward disturbance dynamo electric fields (DDEF) [27].

The event 5, (7 October 2015) is found to be exhibited a totally different variation. itshowed a very less positive storm effectsas sharply reduced VTEC and EIA suppression caused by westward electric field penetration and a drop in the O/N_2 ratio, and downward plasma motion.The TEC are more enhanced in specific marked region it may be due to redistribution of ionospheric plasma. A study on the effects of the strong storm on 7 October, 2015, and the severe magnetic storm on 17 March, 2015, on the ionosphere across the low-latitude areas of Saudi Arabia was carried out by the Sharma et al. (2020). Their results show a negative storm effect by the storm on 7 October, which had a minimum Dst of -124 nT and an Auroral Electrojet (AE) enhancement up to 1209.30 nT. This resulted in a considerable fall in VTEC of -72.14% when compared to ordinary quiet days. The suppression of the equatorial ionisation anomaly, which results in a downward shift of the F2 layer, a reduction in hmF2, and a depletion of the O/N2 ratio, is most likely the cause of the observed fall in VTEC during the main phase of the storm. In addition, during the storm period, there was increased amplitude scintillation across the low-latitude regions, the intensity of this scintillation was correlated with the storm's severity[28].

It is well known that while geomagnetic storms have a significant and dominant impact on TEC variability, other natural activities such as earthquakes can also induce localized TEC perturbations, though their effects are generally minor in comparison. Due to this reason, we also examined global earthquake catalogs for the periods of the selected storm events. Specifically, we checked for significant seismic events ($Mw \geq 5.0$) within a radius of ~1000 km around the IGS stations. Our analysis confirmed that no such earthquakes occurred during the considered intervals. Hence, the TEC anomalies presented in this study may be highly attributed to geomagnetic storm activity rather than seismic influences.

4 Conclusion

The examination of TEC fluctuations during several geomagnetic storms spanning from 2012 to 20[21]at six IGS stations (GUAM, GUUG, IISC, DARW, KAT1, and ALIC) reveals substantial disturbances in the ionosphere directly associated with geomagnetic activity. Specifically, the storms in September 2017, March 2015, and December 2015 displayed significant deviations in VTEC, indicating notable increases in TEC values and percentage changes, especially at ALIC and KAT1 stations. These occurrences highlight the substantial Geomagnetic

storms' effects on ionospheric conditions, driven by mechanisms like PPEFs and the EEJ, which result in heightened electron densities and TEC values in affected areas. The global TEC maps during these events also demon strated the spatial variability of ionospheric responses, with elevated TEC values predominantly noticed in low-latitude and equatorial areas. The disparities in TEC enhancements across different regions underscore the intricate interplay between geomagnetic disturbances and local ionospheric conditions, influenced by factors such as geomagnetic latitude, local time, and solar radiation. These results emphasize how important it is to track global TEC fluctuations in order to gain a greater understanding of how space weather events may affect the ionosphere. The outcomes contribute to the broader understanding of how geomagnetic storms influence ionospheric dynamics, emphasizing the necessity for continuous observation and analysis to mitigate potential impacts on satellite-based technologies and communication systems.

References

1 Gold T, *Space Sci Rev*, 1 (1962) 100, doi: 10.1007/ BF00174637.

2 Piddington J H, *Space Sci Rev*, 3 (1964) 724, https://doi.org/10.1007/BF00177956.

3 Akasofu S I, *Space Sci Rev*, 164 (2011) 85, https://doi.org/ 10.1007/s11214-011-9856-y.

4 Lakhina G S & Tsurutani B T, *Geosci Lett*, 3 (2016) 1, https://doi.org/10.1186/s40562-016-0037-4.

5 Albertson V D, Bozoki B, Feero W E, Kappenman J G, Larsen E V, Nordell D E & Walling R, *IEEE Trans Power Deliv*, 8 (1993) 1206.

6 Lanzerotti L J, *Geophys Monogr Ser*, 125 (2001) 11, https://doi.org/10.1029/GM125p0011.

7 McManus D J, Carr H H & Adams B M, *Int J Interact Mob Technol*, 5 (2011) 3, DOI:10.3991/ijim.v5i3.1667.

8 Appleton E V, *Nature*, 157 (1946) 691, https://doi.org/10. 1038/157691a0

9 da Costa A M, Boas J W V & da Fonseca E S, *Geofis Int*, 43 (2004) 129, DOI:10.22201/igeof.00167169p.2004.43.1.224.

10 Fejer B G, *J Atmos Terr Phys*, 53 (1991) 677, https://doi.org/ 10.1016/0021-9169(91)90121-M.

11 Woodman R F & La Hoz C, *J Geophys Res*, 81 (1976) 5447, https://doi.org/10.1029/JA081i031p05447.

12 Trivedi R, Jain A, Jain S & Gwal A K, *Adv Space Res*, 48 (2011) 1617, https://doi.org/10.1016/j.asr.2011.08.008.

13 Oikonomou C, Haralambous H, Paul A, Ray S, Alfonsi L, Cesaroni C & Sur D, *Adv Space Res*, 70 (2022) 1104, https://doi.org/10.1016/j.asr.2022.05.035.

14 Lissa D, Venkatesh K, Prasad D S V V D & Niranjan K, *Adv Space Res*, 70 (2022) 1089, DOI:10.1016/ J.ASR.2021. 04.021.

15 Tariq M A, Yuyan Y, Shah M, Shah M A, Iqbal T & Liu L, *Adv Space Res*, 70 (2022) 3731, DOI:10.1016/ j.asr.2022.08.050.

16 Jenan R, Dammalage T L & Panda S K, *Acta Astronaut*, 180 (2021) 575, https://doi.org/10.1016/j.actaastro.2021.01.006.

17 Marković M, *Geonauka*, 2 (2014) 1, DOI: 10.14438/ gn. 2014.22.

18 Stankov M S & Muhtarov P Y, *C R Acad Bulg Sci*, 54 (2001) 9.

19 Rangarajan G K & Barreto L M, *Earth Planets Space*, 51 (1999) 363, https://doi.org/10.1186/BF03352240.

20 Sugiura M, *IAGA Bull*, 40 (1991) 17.

21 Gil A M, Renata M, Szczepan S, Agnieszka S M, Wawrzynczak A, Pozoga M & Tomasik L, *Sol Phys*, 295 (2020) 135, DOI:10.1007/s11207-020-01703-2.

22 Paul B, Gordiyenko G & Galav P, *Astrophys Space Sci*, 365 (2020) 174, https://doi.org/10.1007/s10509-020-03884-5.

23 Sharma S, Galav P, Dashora N, Alex S, Dabas R S & Pandey R, *J Geophys Res Space Phys*, 116 (2011) A5, doi:10.1029/2010JA016368, 2.

24 Galav P, Sharma S & Pandey R, *Astrophys Space Sci*, 337 (2012) 543, https://doi.org/10.1007/s10509-011-0869-5.

25 Lissa D, Srinivasu V K D, Prasad D S V V D & Niranjan K, *Adv Space Res*, 66 (2020) 1427, https://doi.org/10.1016/ j.asr.2020.05.025.

26 Mansilla G A & Zossi M M, *Adv Space Res*, 65 (2020) 2083, https://doi.org/10.1016/j.asr.2019.09.025.

27 Amaechi P O, Oyeyemi E O & Akala A O, *Adv Space Res*, 61 (2018) 2074, https://doi.org/10.1016/j.asr.2018. 01.035.

28 Sharma S K, Singh A K, Panda S K & Ahmed S S, *Astrophys Space Sci*, 365 (2020) 35, https://doi.org/ 10.1007/ s10509-021-04036-z.